Since January 2020 Elsevier has created a COVID-19 resource centre with free information in English and Mandarin on the novel coronavirus COVID-19. The COVID-19 resource centre is hosted on Elsevier Connect, the company's public news and information website.

Journal of Molecular Structure 1234 (2021) 130152

Contents lists available at ScienceDirect

Journal of Molecular Structure

journal homepage: www.elsevier.com/locate/molstr

Inhibitory efficacy of RNA virus drugs against SARS-CoV-2 proteins: An extensive study

Manab Mandal[a], Swapan Kumar Chowdhury[b], Abdul Ashik Khan[c], Nabajyoti Baildya[d], Tanmoy Dutta[e], Debabrata Misra[b], Narendra Nath Ghosh[f,*]

[a] Department of Botany, Dukhulal Nibaran Chandra College, Suti 742201, India
[b] Plant and Microbial Physiology and Biochemistry Laboratory, Department of Botany, University of Gour Banga, Malda 732103, India
[c] Department of Chemistry, Darjeeling Govt. College, Darjeeling 734101, India
[d] Department of Chemistry, University of Kalyani, Kalyani 741235, India
[e] Departments of Chemistry, JIS College of Engineering, Kalyani 741235, India
[f] Department of Chemistry, University of Gour Banga, Mokdumpur, Malda 732103, India

ARTICLE INFO

Article history:
Received 10 January 2021
Revised 6 February 2021
Accepted 9 February 2021
Available online 26 February 2021

Keywords:
SARS-CoV-2
RNA virus drugs
Molecular dynamics simulation
Baloxavir marboxil

ABSTRACT

Herein we have made a comprehensive analysis of inhibitory efficacy of 16 RNA virus drugs against RdRp, Mpro and PLpro proteins of SARS-CoV-2. Analysis of docked conformation revealed that Baloxavir marboxil (BMX) corresponds to the highest binding energy. Analysis of residue confirmed that BMX strongly interact with these three proteins involving H-bonding, ionic as well as hydrophobic interactions. Molecular dynamics simulation and analysis of parameters like RMSD, RMSF, binding energy confirmed noticeable conformational alternation with these proteins with makeable effect on RdRp. The potentially inhibitory action of BMX against these three proteins suggests the inhibition of overall transcription process of SARS-CoV-2. These observation along with the recently observed inhibitory action of BMX on influenza with clinically proven no side effects emphasizes to uncover the role of BMX by *in-vitro* and *in-vivo* analysis.

1. Introduction

The recent pandemic COVID-19 causes a Public Health Emergency of International Concern (PHEIC) and seriously damaged the global economy. On January 13th, 2020 complete genome analysis was performed and revealed a novel corona virus (Gen Bank No. MN908947), official name is SARS-CoV-2 previously known as SARS-CoV [1]. SARS-CoV-2 can spread with human-to-human transmission via respiratory droplets (e.g. through coughing or sneezing) or even by contact with contaminated surfaces [2].

It is a single-stranded positive-sense RNA (ssRNA) virus consisting of 29,903 nucleotides and two untranslated sequences of 254 and 229 nucleotides at the 5′- and 3′- ends, respectively and is included in β–corona virus genus, closely related to the genomic organization of SARS-CoV identified in 2003 [3]. The most important structural proteins of CoV are spike (S) protein (trimeric), membrane (M) protein, envelop (E) protein, and the nucleocapsid (N) protein. Some of the viruses such as beta-CoVs also have hem agglutinin esterase (HE) glycoprotein [4]. The interaction of angiotensin converting enzyme 2 (ACE2) of Human cell with spike protein of SARS-CoV-2 helps the virus to enter into the human cell immediately viral replication and transcription are started with the functional proteins like main protease (Mpro), papain-like protease (PLpro), RNA-dependent RNA polymerase (RdRp) [5,6]. Different studies revealed that the viral proteins showed varying mutation rates [7]. NSP12 (RdRp) accompanied with D614G (S) mutation showed mutation rate (MR) 0.994 while other residues of RdRp showed slower mutation rate (MR) 0.04 with A185 and 0.04 with V776 [8].

But till now any potentially active drug is not available in the market to combat with SARS-CoV-2. According to World Health organisation there are 24 vaccines that are in advance stages and another 142 vaccines are also in various early stages of development of the SARS-Cov2 pathogen [9]. Drug repurposing is an excellent way to choose a drug, developed for the treatment of other diseases to treat a new type of disease. But a number of antiviral drugs such as arbidol [10], chloroquine [11], darunavir [12], favipiravir [13], hydroxychloroquine [14], interferons [15], lopinavir [16],

* Corresponding author at: Department of Chemistry, University of Gour Banga, Malda 732103, India.
E-mail address: ghosh.naren13@gmail.com (N.N. Ghosh).

https://doi.org/10.1016/j.molstruc.2021.130152
0022-2860/

Table 1
Docking scores of RNA virus drugs against RdRp, Mpro and PLpro.

Name of the Drugs	Structure of the drugs	Pubchem CID	MW (g/mol)	MF	Docking Score (Kcal/mol)		
					RdRp	Mpro	PL- pro
Adapromine	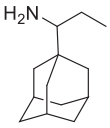	547,499	193.33	$C_{13}H_{23}N$	−5.2	−4.8	−5.2
Amantadine	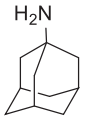	2130	151.25	$C_{10}H_{17}N$	−4.8	−4.3	−4.7
Baloxavir marboxil	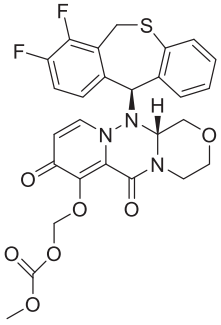	124,081,896	571.6	$C_{27}H_{23}F_2N_3O_7S$	−9.3	−7.8	−7.1
Favipiravir	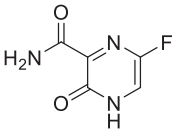	492,405	157.1	$C_5H_4FN_3O_2$	−5.4	−4.8	−5.4
Galidesivir	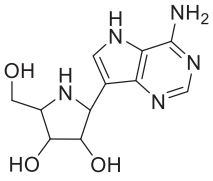	10,445,549	265.27	$C_{11}H_{15}N_5O_3$	−6.5	−7.1	−5.9
Lumicitabine	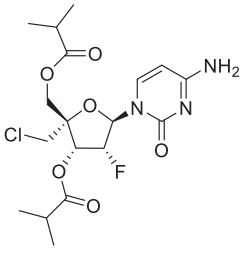	89,658,382	433.9	$C_{18}H_{25}ClFN_3O_6$	−6.9	−6.9	−5.9
Mericitabine	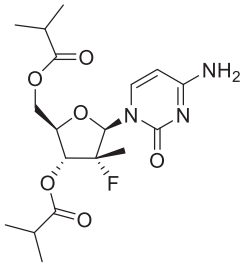	16,122,663	399.4	$C_{18}H_{26}FN_3O_6$	−6.9	−7.3	−5.5

(*continued on next page*)

Table 1 (*continued*)

Name of the Drugs	Structure of the drugs	Pubchem CID	MW (g/mol)	MF	Docking Score (Kcal/mol)		
					RdRp	Mpro	PL- pro
Merimepodib	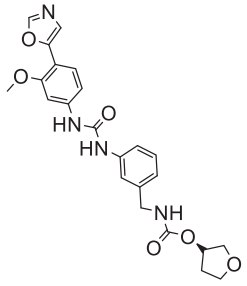	153,241	452.5	$C_{23}H_{24}N_4O_6$	−7.3	−7.6	−7.0
Moroxydine	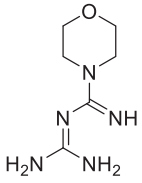	71,655	171.2	$C_6H_{13}N_5O$	−5.8	−5.7	−5.8
Mozenavir	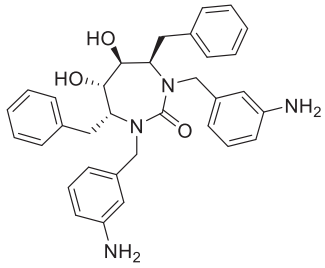	154,044	536.7	$C_{33}H_{36}N_4O_3$	−7.9	−7.4	−6.9
Pleconaril	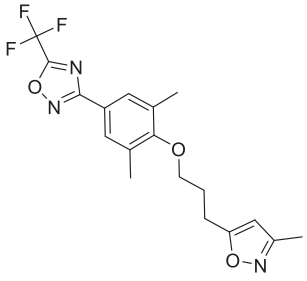	1684	381.3	$C_{18}H_{18}F_3N_3O_3$	−7.1	−7.5	−6.7
Remdesivir	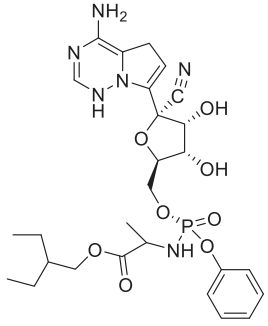	121,304,016	602.6	$C_{27}H_{35}N_6O_8P$	−8.0	−7.8	−6.3
Ribavirin	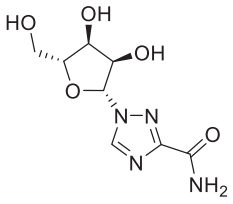	37,542	244.2	$C_8H_{12}N_4O_5$	−6.7	−6.1	−5.7

(*continued on next page*)

Table 1 (*continued*)

Name of the Drugs	Structure of the drugs	Pubchem CID	MW (g/mol)	MF	Docking Score (Kcal/mol)		
					RdRp	Mpro	PL- pro
Taribavirin	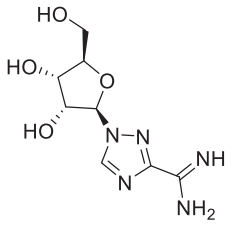	451,448	243.22	$C_8H_{13}N_5O_4$	−6.9	−6.1	−6.0
Umifenovir	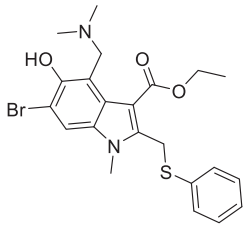	131,411	477.4	$C_{22}H_{25}BrN_2O_3S$	−6.9	−6.5	−5.2
Valopicitabine	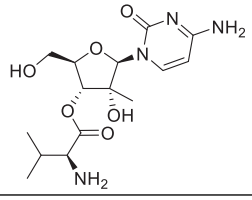	6,918,726	356.37	$C_{15}H_{24}N_4O_6$	−6.0	−6.6	−5.6

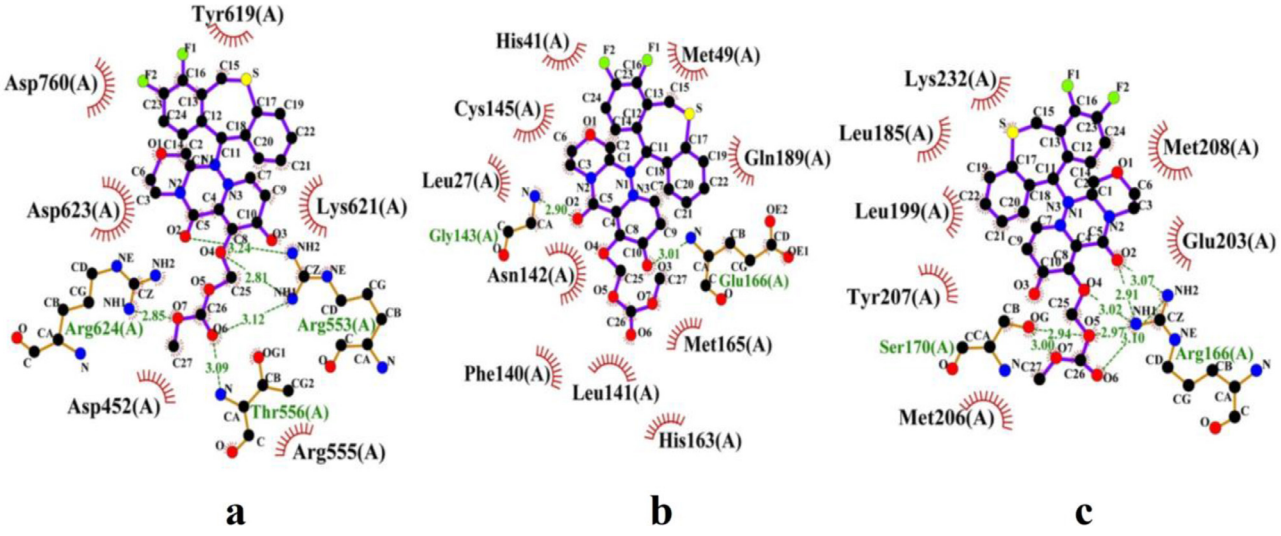

Fig. 1. Docked conformations of (a) RdRp-BMX, (b) Mpro-BMX and (c) PLpro-BMX with respective neighbours (all H-bond distances are in Å unit).

oseltamivir [17], remdesivir [18], cefpiramide [19], ribavirin [20], ritonavir [16], and tocilizumab [21] are used as treatments for influenza, SARS, MERS, HIV, and malaria and also shown inhibitory effects against the SARS-CoV-2. The antiviral drugs viz. favipiravir strongly inhibits RNA-dependent RNA polymerase (RdRp) viruses, remdesivir inhibits viral RNA polymerases, oseltamivir, lopinavir-ritonavir, ivermectin and interferon alfa-2B inhibit viral replication whearas ribavirin and sofosbuvir inhibiting RNA synthesis [22]. Using the traditional knowledge of viral pathogenesis, pharmacodynamics of drugs [23], different synthetic compounds [24] and using of computational tools many drugs are currently in pipeline to be repurposed for combating the SARS-CoV-2 [22]. Again following the same techniques different plant extracts are used for the treatment of COVID-19 [25,26].

In this study we have selected 16 anti-RNA drugs for virtual screening against RdRp, Mpro and PLpro proteins of SARS-CoV-2. Molecular docking study has been done with the drugs against these three proteins. Highest binding energy and conformational changes were observed. Molecular dynamics simulation was also performed to check the stability of Mpro, PLpro and RdRp protein with the drug by evaluating different parameters like SASA, RMSF, RMSD, radius of gyration analysis.

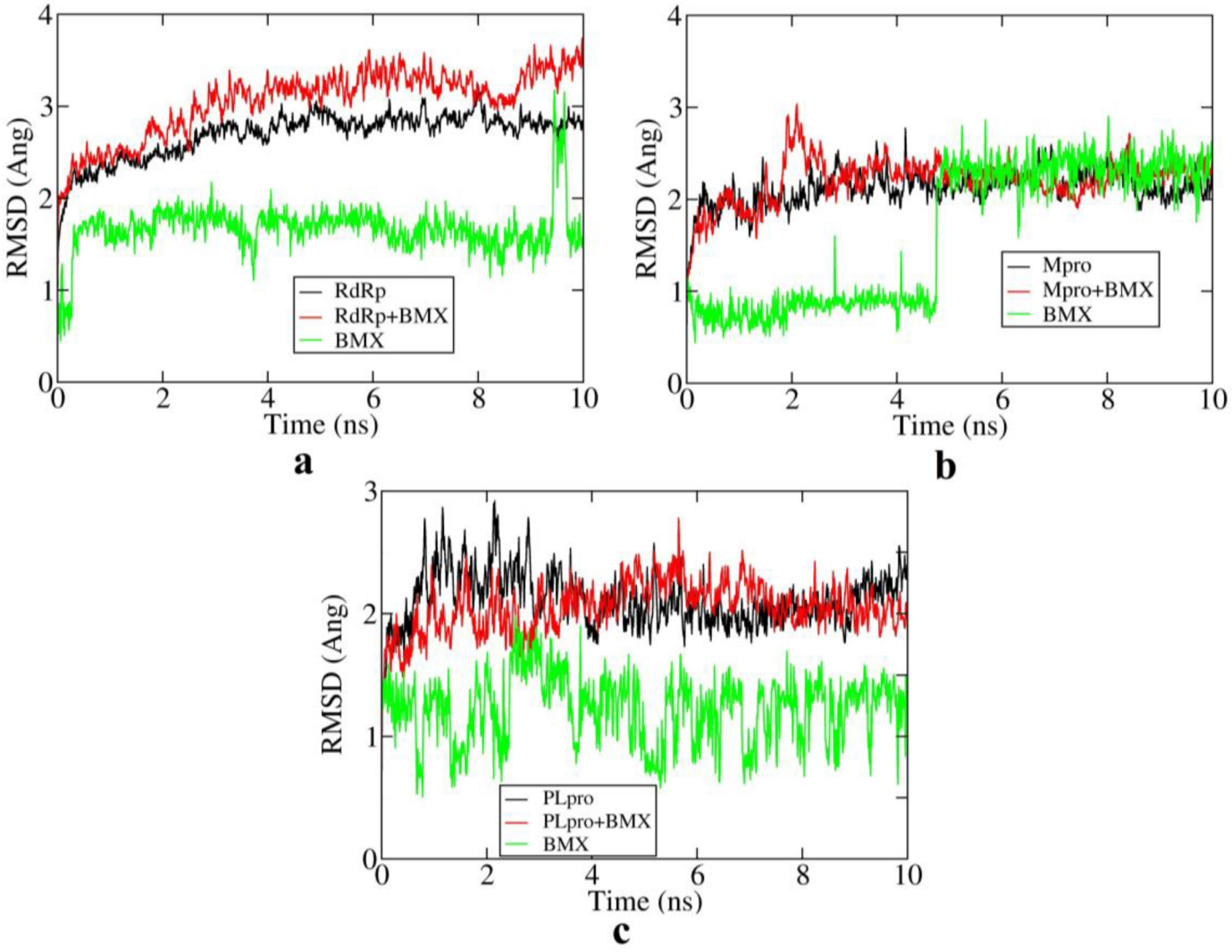

Fig. 2. RMSD plots for docked and undocked (a) RdRp, (b) Mpro and (c) PLpro.

2. Methodology

2.1. Molecular docking studies

The crystal structures of SARS-CoV-2 RdRp (PDB ID: 6M71), Mpro (PDB ID: 6LU7) and PLpro (PDB ID: 6W9C) were obtained from protein data bank (http://www.rcsb.org). Autodock tools was used to clean the structure by removing heteroatoms and by adding necessary hydrogen atoms. The structures of the 16 drug molecules were obtained from PubChem. The pdb files of the drugs were created using UCSF Chimera [27] for docking and the docking between the drugs and selected proteins at their best binding sites were performed by using Autodock Vina [28] package.

2.2. Molecular dynamics (MD) simulation studies

10 ns MD-simulation was performed with the minimum energy conformer of the proteins and Baloxavir marboxil (BMX) complex using Gromacs (5.1) [28] with CHARMM36-march2019 force field [29]. The TIP3P water model [30] was used for solvation. Drug (BMX) parameter and topology files were generated by using CGenFF server. A cubical box with a buffer dimension $10 \times 10 \times 10$ Å^3 was created and adequate number of ions were added to maintain electro neutrality. A 100 ps NVT and NPT equilibration were performed with the complex by keeping 2 fs time step after performing energy minimization of the complexes to 10 kJmol^{-1}nm^{-1}. Particle mesh Ewald (PME) method were applied for the calculation of long range interactions. Finally 10 ns MD simulations with the equilibrated ensembles were performed using same cut-off. A modified Berendsen thermostat and a Parinello-Rahman barostat were used with reference temperature and pressure at 300 K and 1 bar respectively. Snapshots of the trajectory were saved every 1 ns for each case.

2.3. Binding free energy calculation

Binding free energies were calculated by molecular mechanics Poison-Boltzmann surface area (MM-PBSA) method [31], implemented on Gromacs tool (g_mmpbsa) [32]. The following formulae

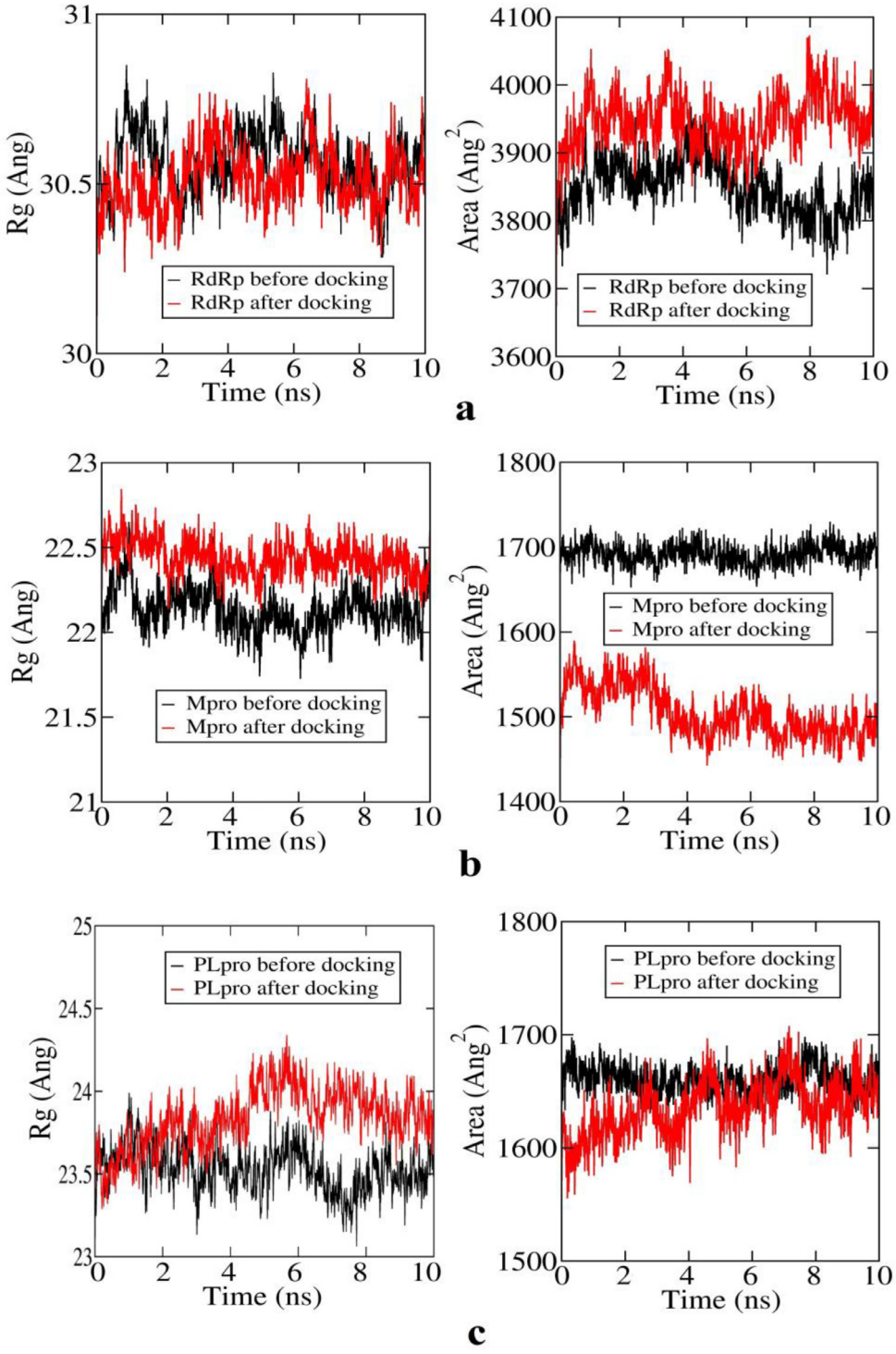

Fig. 3. Radius of gyration (left panel) and SASA (right panel) plot for RdRp, Mpro and PLpro in docked and undocked form.

were used to calculate the binding energies.

$$\mathbf{\Delta G_{bind} = G_{w-complex} - G_{w-protein} - G_{w-drug}} \quad (1)$$

$$\mathbf{G_{w-complex} = \langle E_{MM} \rangle + \langle G_{sol} \rangle - -TS} \quad (2)$$

$$\mathbf{E_{MM} = E_{bonded} + E_{non-bonded} = E_{bonded} + (E_{vdW} + E_{elec})} \quad (3)$$

$$\mathbf{G_{sol} = G_{polar} + G_{non-polar} = G_{polar} + (\gamma SASA + b)} \quad (4)$$

Where, $G_{w\text{-}complex}$ is the total free energy of the protein and drug complex, $G_{w\text{-}protein}$, $G_{w\text{-}drug}$ are the free energies of the protein and drug respectively. E_{MM} is the average MM potential energy including bonding, non-bonding energies, G_{sol} is the free energy of solvation including polar and non-polar energies. SASA is the solvent accessible surface area, γ is the coefficient of surface tension of

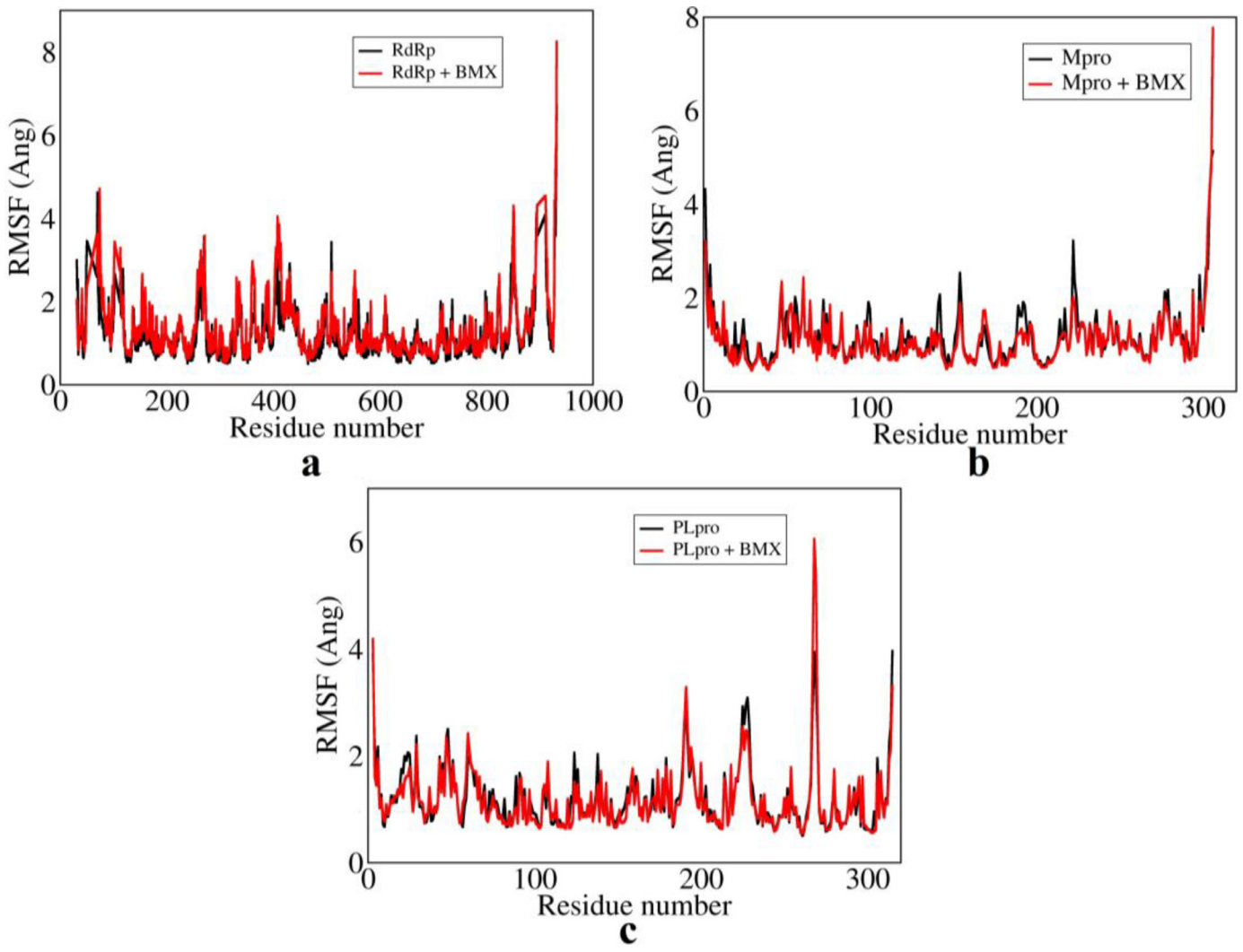

Fig. 4. RMSF plots for docked and undocked RdRp, Mpro and PLpro.

Table 2
Different types of interaction energies between proteins and BMX.

Protein-BMX complex	van der Waal energy (kJ/mol)	Electrostattic energy (kJ/mol)	Polar solvation energy (kJ/mol)	SASA energy (kJ/mol)	Binding energy (kJ/mol)
RdRp-BMX	−97.912	−31.048	104.260	−12.551	−37.251
Mpro-BMX	−136.862	−63.268	149.819	−16.019	−66.330
PLpro-BMX	−115.008	−17.814	86.919	−13.162	−59.066

solvent and b is the fitting parameter. TS is not considered by g_mmpbsa.

2.4. Results and discussion

To study the binding interaction of the selected 16 compounds with the RdRp, Mpro and PLpro molecular docking were performed and the initial coordinates are used for further MD calculations. The binding affinities are tabulated in Table 1. We find that among all the compounds, Baloxavir marboxil (BMX) showed highest binding affinities with RdRp (−9.3 Kcal/mol), Mpro (−7.8 Kcal/mol) and PLpro (−7.1 Kcal/mol). It is interesting to note that BMX achieved higher docking affinities with respect to standard reference remdesivir. Previous experimental studies revealed that BMX is unique which inhibit viral replication by forming complex with viral polymerase thereby reduces the activity of RdRp [33,34] which supports our theoretical observations.

The binding mode of BMX with RdRp, Mpro and PLpro proteases are illustrated in Fig. 1. As shown in Fig. 1 BMX formed 5 H-bonds with ARG624, THR556, ARG553 residues of RdRp, 2 H-bonds with GLY 143, GLU166 residues of Mpro and 6 H-bonds with SER170, ARG166 residues of PLpro respectively. The nearest residues are shown in 3D and 2D contour plot in Fig. S1 along with respective H-bonds.

2.5. ADMET analysis

ADMET (i.e. Absorption, Distribution, Metabolism, Excretion, and Toxicity) profiling of the compounds were performed with the help of pkCSM online server [35]. All the studied compounds

Table 3
Different types of BMX-protein interactions.

System	H-Bond interactions	π-Stacking	Hydrophobic Interactions
RdRp_BMX	553ARG, 556THR, 624ARG	–	–
Mpro_BMX	143GLY, 144SER, 145CYS, 166GLU	–	142ASN
PLpro_BMX	166ARG, 170SER	207TYR, 232LYS	199LEU, 207TYR

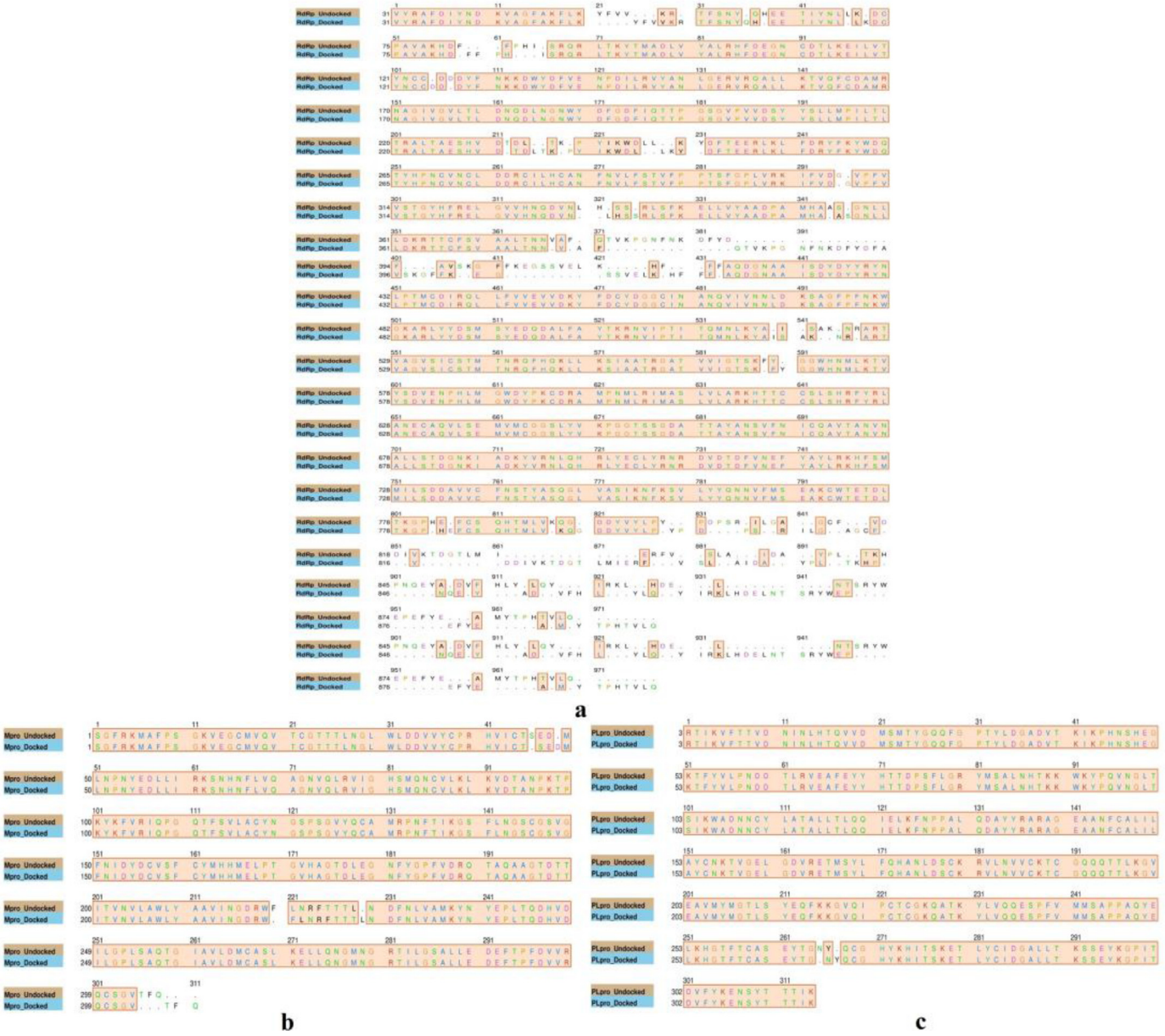

Fig. 5. Conformational changes in (a) RdRP, (b) Mpro and (c) PLpro after MD-simulation before and after docking.

have a skin permeability ranging from −3.280 to −2.524. Most of the drugs do not inhibit P-glycoprotein I and II. Blood-brain barrier (BBB) permeability and CNS permeability values are laying between −2.056 to +0.867 and −5.158 to −1.849 respectively. Most of them also do not inhibit CYP1A2, CYP2C19, CYP2C9, CYP2D6, CYP3A4 inhibitors and they do not interact with renal OCT2 substrate. These data are tabulated in Table S1. Along with that most of the drugs neither show AMES toxicity nor inhibit hERGI inhibitor.

To uncover the conformational dynamics of these three systems of RdRp_BMX, Mpro_BMX and PLplo_BMX the root mean square deviations (RMSD) were calculated from the energy minimized structures derived from molecular docking studies.

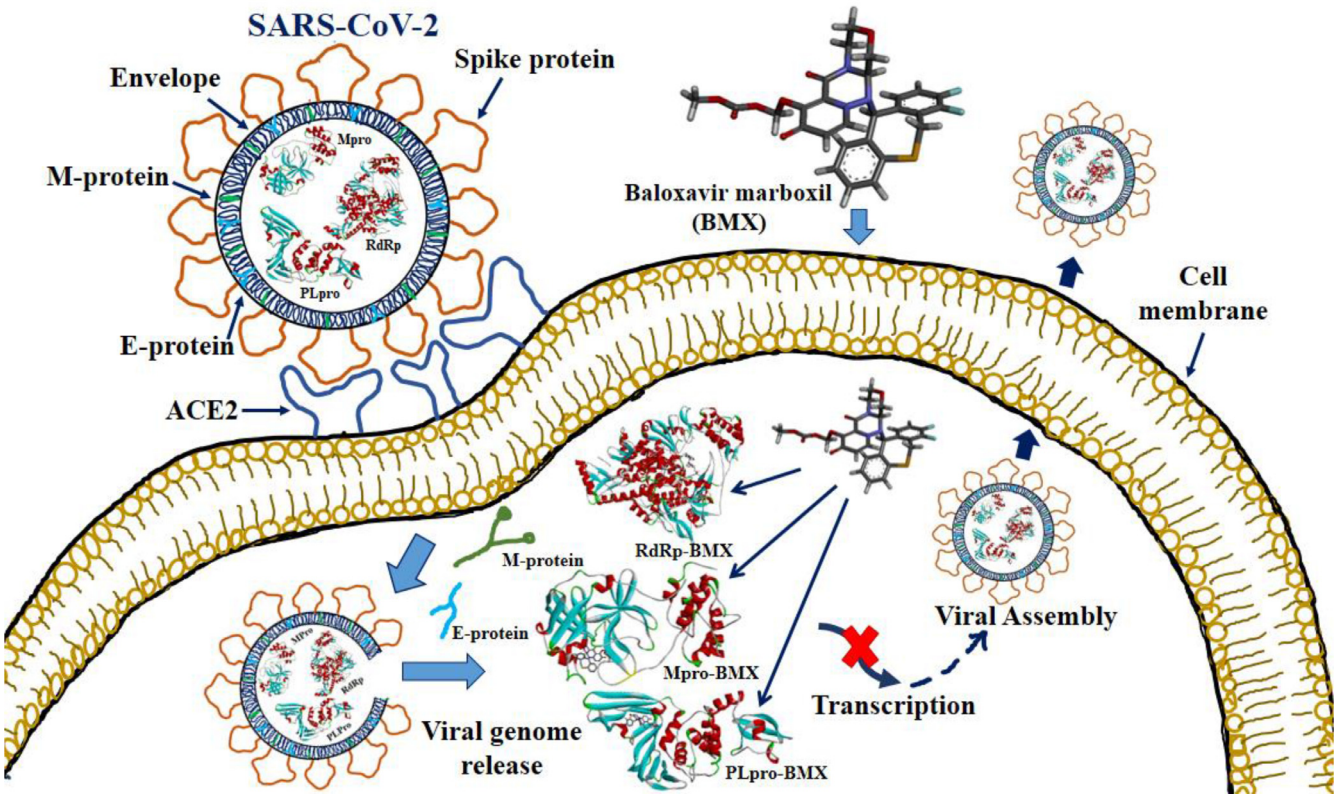

Fig. 6. Mechanism of action of BMX on SARS-CoV-2 proteins.

The RMSD plots of individual protein and the docked one are shown in Fig. 2. One most common interesting thing with all RMSD plots is that the three docked complexes were achieved equilibrium within a very short time of 1 ns and fluctuated with a RMSD value around 3.7 Å for RdRp_BMX, 3 Å for Mpro_BMX and 2.5 Å PLpro_BMX suggesting that BMX is able to bind the corresponding proteins very quickly. Lesser fluctuation RMSD in case of PLpro_BMX complex indicates the strong binding between PLpro and BMX compared to other proteases.

The compactness of a system is measured by radius of gyration. Fig. 3 showed the radius of gyration plot for RdRp, Mpro and PLpro in docked and undocked form. All the three plots for radius of gyration clearly indicates that there are loss in compactness in presence BMX in three proteins and with the progression of MD this loss in compactness is increased which is in good agreement with the RMSD and radius of gyration plots.

To understand the interaction between proteins and BMX moiety we have performed binding energy calculations which is shown in Table 2. From Table 2 it is clear that binding energies follow the order of Mpro> PLpro> RdRp. There were strong van der Waal, electrostatic interactions between Mpro and BMX compared to RdRp and PLpro.

Furthermore to check the conformational changes after binding with the drug moiety and to analyze the mobility of protein residue average RMSF of each system was calculated. RMSF plots of BMX-protein composites are shown in Fig. 4 which revealed that the residual fluctuation of the docked proteins are quite low with respect to undocked one, confirming strong interaction with the selective residue LYS621, ASP623, ARG624, ARG553, PHE506, ASN507, TRP509, GLY510, TYR122 of RdRp, LEU27, CYS145, ASN142, MET165, GLU166, SER113, VAL114, LEU115, ALA116, TYR118, PRO122 of Mpro and LEU185, LEU199, SER170, ARG166, ILE123, GLU124, LEU125, TYR137, CYS224, THR225 of PLpro with BMX drug. The average RMS fluctuation for Mpro is quite less (1.7 Å) with respect to RdRp (3.6 Å) and PLpro (2 Å) supports stronger binding affinity with Mpro followed by PLpro and RdRp.

Fig. 5 represents the sequence analysis of undocked and docked RdRp, Mpro and PLpro. Here we note that there is a substantial conformational alternation on amino acids residues in three proteins before and after docking. Residue numbers from 21 to 30, 411 to 430 and 931 to 971 of RdRp, 306 to 311 of Mpro and 365 to 367 of PLpro were mostly affected which indicates that BMX has a robust effect on the conformation of RdRp. Table 3 lists different kinds of interactions occurring between BMX and protein moieties.

These results are further confirmed by large fluctuation of the RMSF values of RdRp_BMX complex and is consistent with the recently reported BMX treatment associated with the influenza virus (RNA polymerase inhibitor) with clinically proven no side effects [36].

The mechanism of action of BMX against these three proteins is illustrated schematically in Fig. 6 showing the inhibitory action of overall transcription process on SARS-CoV-2. During the MD-simulation snapshots of conformational changes are captured and are represented in Fig. 7. Profound conformational changes are noticed after 3 ns for three docked composites and with Mpro these changes are significant which is also confirmed from their RMSD and RMSF plots.

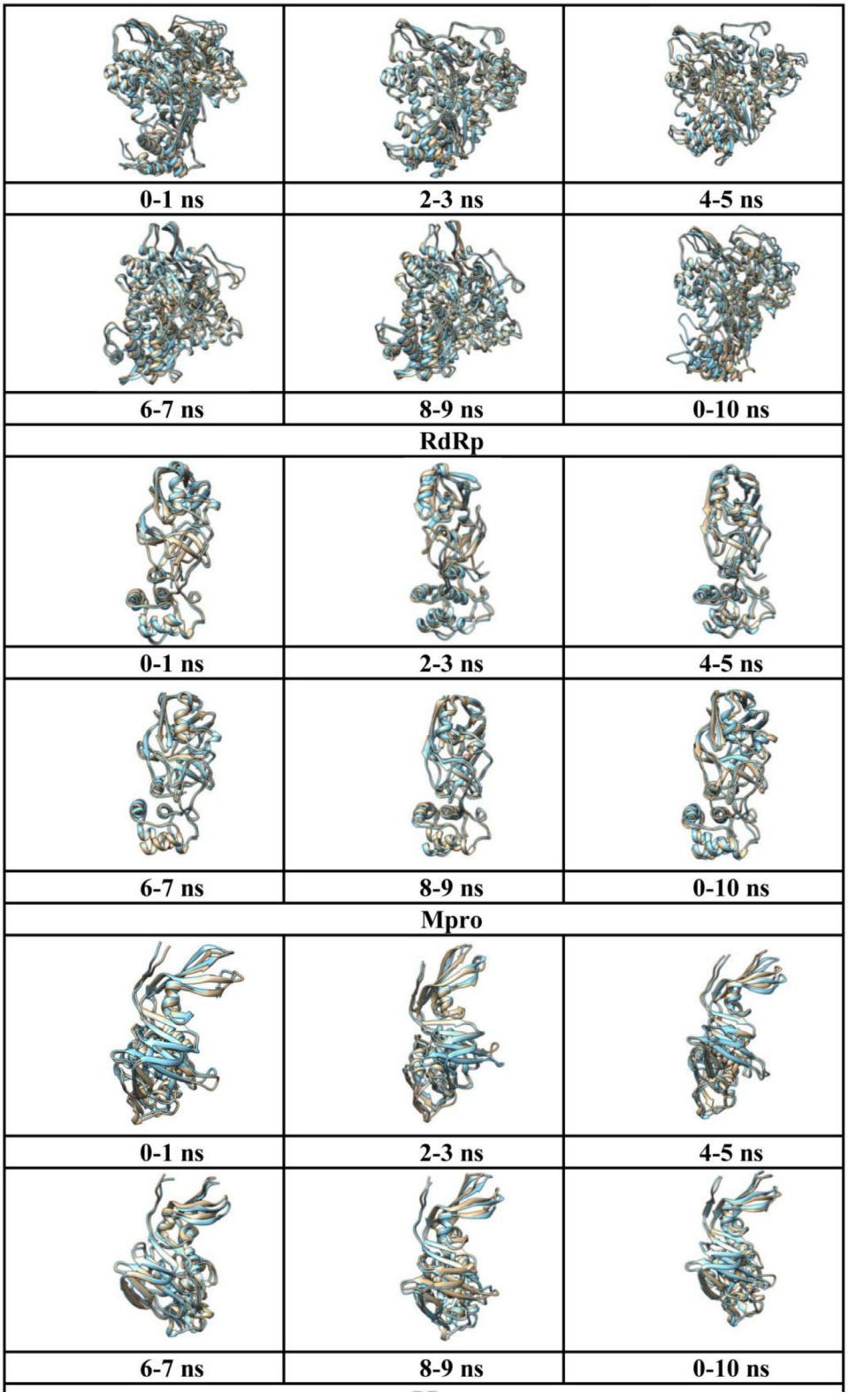

Fig. 7. Conformational changes of RdRp, Mpro and PLpro during MD-simulation.

3. Conclusions

The present study computationally probed 16 RNA virus drugs for prediction of their potential inhibitory activities against RdRp, Mpro and PLpro proteins of coronavirus. Analysis of favourable docked conformations of studied compounds revealed that BMX has the highest binding affinity with these three proteins. Residue analysis revealed that BMX strongly interact with these three proteins involving H-bonding, ionic as well as hydrophobic interactions. MD-simulation and evaluation of parameters like RMSD, RMSF and residue analysis of protein before and after docking revealed that BMX has a profound effect on the conformational alter-

nation with these three proteins with noticeable emphasizing effect specially on RdRp. Our present observation is consistent with the recently reported BMX treatment associated with the influenza virus (RNA polymerase inhibitor) with clinically proven no side effects. Analysis of all the parameters supports that BMX has potential inhibitory activity against RdRp, Mpro and PLpro of SARS-CoV-2 making it available for intimate *in-vivo* and *in-vitro* testing.

Declaration of Competing Interest

The Authors declare that they have no conflict of interest.

Supplementary materials

Supplementary material associated with this article can be found, in the online version, at doi:10.1016/j.molstruc.2021.130152.

CRediT authorship contribution statement

Manab Mandal: Formal analysis, Validation. **Swapan Kumar Chowdhury:** Conceptualization, Formal analysis. **Abdul Ashik Khan:** Conceptualization, Validation. **Nabajyoti Baildya:** Validation, Writing - review & editing, Software. **Tanmoy Dutta:** Validation, Formal analysis, Writing - review & editing. **Debabrata Misra:** Validation, Writing - review & editing. **Narendra Nath Ghosh:** Supervision, Writing - review & editing, Software.

References

[1] W.H. Organization, Coronavirus disease (COVID-2019) situation reports. 2020, Available on: https://www.WHO.Int/docs/default-source/coronaviruse/situationreports/20200221-sitrep-32-covid19 (2020).
[2] S.Y. Shahin, A.S. Bugshan, K.S. Almulhim, M.S. AlSharief, Y.A. Al-Dulaijan, I. Siddiqui, F.D. Al-Qarni, Knowledge of dentists, dental auxiliaries, and students regarding the COVID-19 pandemic in Saudi Arabia: a cross-sectional survey, BMC Oral Health 20 (1) (2020) 1–8.
[3] M. Pal, G. Berhanu, C. Desalegn, V. Kandi, Severe acute respiratory syndrome Coronavirus-2 (SARS-CoV-2): an update, Cureus 12 (3) (2020).
[4] H. Zhang, J.M. Penninger, Y. Li, N. Zhong, A.S. Slutsky, Angiotensin-converting enzyme 2 (ACE2) as a SARS-CoV-2 receptor: molecular mechanisms and potential therapeutic target, Intensive Care Med. 46 (4) (2020) 586–590.
[5] Y. Indwiani Astuti, Severe Acute Respiratory Syndrome Coronavirus 2 (SARS–CoV-2): an overview of viral structure and host response, Diabetes Metab Syndr. (2020).
[6] A.K. Dutta, Vaccine against Covid-19 Disease–present status of development, Indian J. Pediatr. (2020) 1–7.
[7] N. Kaushal, Y. Gupta, M. Goyal, S.F. Khaiboullina, M. Baranwal, S.C. Verma, Mutational frequencies of SARS-CoV-2 genome during the beginning months of the outbreak in USA, Pathogens 9 (7) (2020) 565.
[8] S. Vilar, D.G. Isom, One year of SARS-CoV-2: how much has the virus changed? Biology (Basel) 10 (2) (2021) 91.
[9] Z. Khan, Y. Karataş, A.F. Ceylan, H. Rahman, COVID-19 and therapeutic drugs repurposing in hand: the need for collaborative efforts, Le Pharmacien Hospitalier et Clinicien (2020).
[10] W. Gao, S. Chen, K. Wang, R. Chen, Q. Guo, J. Lu, X. Wu, Y. He, Q. Yan, S. Wang, Clinical features and efficacy of antiviral drug, Arbidol in 220 nonemergency COVID-19 patients from East-West-Lake Shelter Hospital in Wuhan: a retrospective case series, Virol. J. 17 (1) (2020) 1–9.
[11] N. Baildya, N.N. Ghosh, A.P. Chattopadhyay, Inhibitory capacity of Chloroquine against SARS-COV-2 by effective binding with Angiotensin converting enzyme-2 receptor: an insight from molecular docking and MD-simulation studies, J. Mol. Struct. (2021).
[12] S. De Meyer, D. Bojkova, J. Cinatl, E. Van Damme, C.B. Meng, M. Van Loock, B. Woodfall, S. Ciesek, Lack of antiviral activity of darunavir against SARS–CoV-2, Int. J. Infect. Dis. (2020).
[13] U. Agrawal, R. Raju, Z.F. Udwadia, Favipiravir: a new and emerging antiviral option in COVID-19, Med. J. Armed Forces India (2020).
[14] N. Baildya, N.N. Ghosh, A.P. Chattopadhyay, Inhibitory activity of hydroxychloroquine on COVID-19 main protease: an insight from MD-simulation studies, J Mol. Struct. (2020) 128595.
[15] E. Sallard, F.-X. Lescure, Y. Yazdanpanah, F. Mentre, N. Peiffer-Smadja, A. Florence, Y. Yazdanpanah, F. Mentre, F.-X. Lescure, N. Peiffer-Smadja, Type 1 interferons as a potential treatment against COVID-19, Antiviral Res. (2020) 104791.
[16] W.-J. Guan, Z.-Y. Ni, Y. Hu, W.-H. Liang, C.-Q. Ou, J.-X. He, L. Liu, H. Shan, C.-l. Lei, D.S. Hui, Clinical characteristics of coronavirus disease 2019 in China, N. Engl. J. Med. 382 (18) (2020) 1708–1720.
[17] Q. Tan, L. Duan, Y. Ma, F. Wu, Q. Huang, K. Mao, W. Xiao, H. Xia, S. Zhang, E. Zhou, Is oseltamivir suitable for fighting against COVID-19: in silico assessment, in vitro and retrospective study, Bioorg. Chem. 104 (2020) 104257.
[18] M.J. Glaus, S. Von Ruden, Remdesivir and COVID-19, Lancet North Am. Ed. 396 (10256) (2020) 952.
[19] A.A. Khan, N. Baildya, T. Dutta, N.N. Ghosh, Inhibitory efficiency of potential drugs against SARS-CoV-2 by blocking human angiotensin converting enzyme-2: virtual screening and molecular dynamics study, Microb. Pathog. (2021) 104762.
[20] J.S. Khalili, H. Zhu, N.S.A. Mak, Y. Yan, Y. Zhu, Novel coronavirus treatment with ribavirin: groundwork for an evaluation concerning COVID-19, J. Med. Virol. (2020).
[21] S.C. Jordan, P. Zakowski, H.P. Tran, E.A. Smith, C. Gaultier, G. Marks, R. Zabner, H. Lowenstein, J. Oft, B. Bluen, Compassionate use of tocilizumab for treatment of SARS-CoV-2 pneumonia, Clin. Infect. Dis. (2020).
[22] C. Harrison, Coronavirus puts drug repurposing on the fast track, Nat. Biotechnol. 38 (4) (2020) 379–381.
[23] M. Karaman, Pharmacophore Analyses of SARS-CoV-2 Active Main Protease Inhibitors Using Pharmacophore Query and Docking Study, (2020).
[24] A. Tan, Novel 1, 2, 3-triazole compounds: synthesis, In vitro xanthine oxidase inhibitory activity, and molecular docking studies, J. Mol. Struct. 1211 (2020) 128060.
[25] B. Benarba, A. Pandiella, Medicinal plants as sources of active molecules against COVID-19, Front. Pharmacol. (2020) 11.
[26] N. Baildya, A.A. Khan, N.N. Ghosh, T. Dutta, A.P. Chattopadhyay, Screening of potential drug from Azadirachta Indica (Neem) extracts for SARS-CoV-2: an insight from molecular docking and MD-simulation studies, J. Mol. Struct. (2020) 129390.
[27] E.F. Pettersen, T.D. Goddard, C.C. Huang, G.S. Couch, D.M. Greenblatt, E.C. Meng, T.E. Ferrin, UCSF Chimera—A visualization system for exploratory research and analysis, J. Comput. Chem. 25 (13) (2004) 1605–1612.
[28] O. Trott, A.J. Olson, AutoDock Vina: improving the speed and accuracy of docking with a new scoring function, efficient optimization, and multithreading, J. Comput. Chem. 31 (2) (2010) 455–461.
[29] S. Lee, A. Tran, M. Allsopp, J.B. Lim, J.r.m. Hénin, J.B. Klauda, CHARMM36 united atom chain model for lipids and surfactants, J. Phys. Chem. B 118 (2) (2014) 547–556.
[30] S. Boonstra, P.R. Onck, E. van der Giessen, CHARMM TIP3P water model suppresses peptide folding by solvating the unfolded state, J. Phys. Chem. B 120 (15) (2016) 3692–3698.
[31] R. Kumari, R. Kumar, O.S.D.D. Consortium, A. Lynn, g_mmpbsa A GROMACS tool for high-throughput MM-PBSA calculations, J. Chem. Inf. Model 54 (7) (2014) 1951–1962.
[32] N.A. Baker, D. Sept, S. Joseph, M.J. Holst, J.A. McCammon, Electrostatics of nanosystems: application to microtubules and the ribosome, Proc. Natl. Acad. Sci. 98 (18) (2001) 10037–10041.
[33] R. O'Hanlon, M.L. Shaw, Baloxavir marboxil: the new influenza drug on the market, Curr. Opin. Virol. 35 (2019) 14–18.
[34] E. Takashita, Influenza polymerase inhibitors: mechanisms of action and resistance, Cold Spring Harb Perspect. Med. (2020) a038687.
[35] D.E. Pires, T.L. Blundell, D.B. Ascher, pkCSM: predicting small-molecule pharmacokinetic and toxicity properties using graph-based signatures, J. Med. Chem. 58 (9) (2015) 4066–4072.
[36] F.G. Hayden, N. Sugaya, N. Hirotsu, N. Lee, M.D. de Jong, A.C. Hurt, T. Ishida, H. Sekino, K. Yamada, S. Portsmouth, Baloxavir marboxil for uncomplicated influenza in adults and adolescents, N. Engl. J. Med. 379 (10) (2018) 913–923.